Int. J. Therm. Sci. (2001) 40, 681–689

S1290-0729(01)01257-1/FLA

Performance comparison of turbines for wave power conversion

Tae-Ho Kim [a], Manabu Takao [b*], Toshiaki Setoguchi [a], Kenji Kaneko [a], Masahiro Inoue [c]

[a] *Department of Mechanical Engineering, Saga University, 1, Honjo-machi, Saga-shi, Saga 840-8502, Japan*

[b] *Department of Control Engineering, Matsue National College of Technology, 14-4, Nishiikuma-cho, Matsue-shi, Shimane 690-8518, Japan*

[c] *Department of Mechanical Science and Engineering, Kyushu University, 6-10-1, Hakozaki, Higashi-ku, Fukuoka-shi, Fukuoka 812-8581, Japan*

(Received 26 July 2000, accepted 25 September 2000)

Abstract — The objective of this paper is to compare the performances of bi-directional turbines under irregular wave condition, which could be used for wave power conversion in the near future. The overall performances in connection with the behavior of oscillating water columns have been evaluated numerically. The types of turbine included in the paper are as follows:

(a) Wells turbine with guide vanes (WTGV);
(b) turbine with self-pitch-controlled blades (TSCB);
(c) biplane Wells turbine with guide vanes (BWGV);
(d) impulse turbine with self-pitch-controlled guide vanes (ISGV), and
(e) impulse turbine with fixed guide vanes (IFGV).

In the study, the experimental investigations were carried out to clarify the performance under steady flow condition and then the numerical simulation was used for predicting the performance of the turbine under irregular wave condition, which typically occurs in the sea. As a result, it is found that the running and starting characteristics of the impulse type turbines could be superior to those of the Wells turbine under irregular wave condition. © 2001 Éditions scientifiques et médicales Elsevier SAS

fluid machinery / Wells turbine / impulse turbine / wave power conversion / ocean energy

Nomenclature

A_c	air chamber cross-sectional area	m^2
AR	aspect ratio	
A_t	turbine flow passage area	m^2
b	blade height	m
C_A	input coefficient (equation (2))	
$\overline{C_i}$	mean input coefficient (equation (13))	
$\overline{C_o}$	mean output coefficient (equation (12))	
C_T	torque coefficient (equation (1))	
f	frequency of wave motion	s^{-1}
$\overline{f}$	mean frequency of wave motion $= 1/\overline{T}$	s^{-1}
f^*	nondimensional frequency $= f/\overline{f}$	
h	wave height in air chamber	m
h^*	nondimensional wave height in air chamber $= h/H_{1/3}$	
H	incident wave height	m
$H_{1/3}$	significant wave height	m
H^*	nondimensional incident wave $= H/H_{1/3}$	
I	moment of inertia of rotor	$kg{\cdot}m^2$
K	nondimensional period $= r_R m/H_{1/3}$	
l	chord length	m
N	number of waves	
m	area ratio $= A_t/A_c$	
Q	flow rate	$m^3{\cdot}s^{-1}$
r_R	mean radius	m
S^*	nondimensional spectrum of wave motion (equation (4))	
S_r	rotor blade space at r_R	m
t	time	s
$\overline{t}^*$	nondimensional time in irregular flow $= t/\overline{T}$	
t_a	width of flow path at r_R	m
T	period of wave motion	s
T_o	output torque	N·m
T_L	loading torque	N·m

* Correspondence and reprints.

E-mail addresses: 99ts12@edu.cc.saga-u.ac.jp (T.-H. Kim), takao@control.matsue-ct.ac.jp (M. Takao), setoguci@me.saga-u.ac.jp (T. Setoguchi), kaneko@me.saga-u.ac.jp (K. Kaneko), ino@mech.kyushu-u.ac.jp (M. Inoue).

$\overline{T}$	mean period in irregular flow $= 1/\overline{f}$	s
U_R	circumferential velocity at r_R	m·s^{-1}
V	reference velocity $= H_{1/3}/(m\overline{T})$	m·s^{-1}
v_a	mean axial flow velocity	m·s^{-1}
v_a^*	nondimensional axial flow velocity $= v_a/V$ (equation (10))	
w	relative inflow velocity	m·s^{-1}
$\overline{W}_i$	incident wave power (equation (7))	W·m^{-1}
$\overline{W}_O$	wave power of OWC (equation (8))	W·m^{-1}
X_I	nondimensional moment of inertia $= I/(\pi\rho_a r_R^5)$	
X_L	nondimensional loading torque $= T_L/(\pi\rho_a V_a^2 r_R^3)$, $T_L/(\pi\rho_a V^2 r_R^3)$	
z	number of rotor blades	

Greek symbols

Δp	total pressure drop between settling chamber and atmosphere	Pa
γ	blade inlet (outlet) angle for impulse turbine rotor	°
δ	camber angle of guide vane	°
$\tilde{\eta}$	conversion efficiency under irregular flow condition (equation (15))	
$\tilde{\eta}_c$	efficiency of air chamber (equation (9))	
$\tilde{\eta}_t$	mean turbine efficiency under irregular flow condition (equation (14))	
θ	setting angle of guide vane	°
ν	hub-to-tip ratio	
λ	sweep angle	°
ρ_a	density of air	kg·m^{-3}
ρ_s	density of seawater	kg·m^{-3}
σ	solidity at $r_R = l \cdot z \cdot (2\pi \cdot r_R)^{-1}$	
ϕ	flow coefficient (equation (3))	
ω	angular velocity of rotor	rad·s^{-1}
$\overline{\omega}^*$	nondimensional angular velocity under irregular flow condition $= \omega\overline{T}$	

Subscripts

g	guide vane
r	rotor
R	mean radius
1	nozzle
2	diffuser

Superscript

$*$	nondimensional value

1. INTRODUCTION

A Wells turbine is a self-rectifying air turbine which is expected to be widely used in wave energy devices with oscillating water columns (OWC). There are many reports that describe the performance of the Wells turbine both at starting and at running conditions [1, 2]. According to these results, the Wells turbine has inherent disadvantages: lower efficiency, poorer starting and higher noise level in comparison with conventional turbines. In order to overcome these weak points, many kinds of turbines have been proposed [3–7]. However, the comparison of characteristics of all these is limited to the turbine characteristics.

The objective of this paper is to compare the performances of turbines in connection with OWC under irregular wave condition, which could be used for wave power conversion in the near future. The types of turbine included in the paper are as follows:

(a) Wells turbine with guide vanes named WTGV in this paper, *figure 1* [3].

(b) Turbine with self-pitch-controlled blades named TSCB, *figure 2* [4].

(c) Biplane Wells turbine with guide vanes named BWGV, *figure 3* [5].

(d) Impulse turbine with self-pitch-controlled guide vanes named ISGV, *figure 4* [6].

(e) Impulse turbine with fixed guide vane named IFGV, *figure 5* [7].

The present status of these turbines is as follows: The Wells turbine with guide vanes was adopted for the project so-called "Mighty Whale" organized by JMSTEC, Japan [8]. The turbine with self-pitch-controlled blades may be connected with the "Azores Pilot Plant" supported from the JOULE II [9], where the turbine has actively pitch-controlled blades. The project using the biplane Wells turbine is making progress in Islay, UK [9], where the guide vanes are not used for the turbine. The impulse turbine with self-pitch-controlled guide vanes has been constructed by NIOT, India [10]. The impulse turbine with fixed guide vane is being planned to be constructed in India, China and Ireland [11].

2. EXPERIMENTAL APPARATUS AND PROCEDURES

The test rig consisted of a large piston-cylinder, a settling chamber and a 300-mm-dia. test section with a bellmouthed entry and a diffuser exit (*figure 6*) [1, 3, 4]. The turbine rotor with $\nu = 0.7$ was placed at the center of the test section and tested at a constant rotational speed under steady flow conditions. The test Reynolds number based on blade chord was about 2.0×10^5 at peak efficiency for WTGV, TSCB and BWGV (Wells type turbines), and 0.4×10^5 for ISGV and IFGV (impulse type turbines). The overall performance was evaluated by

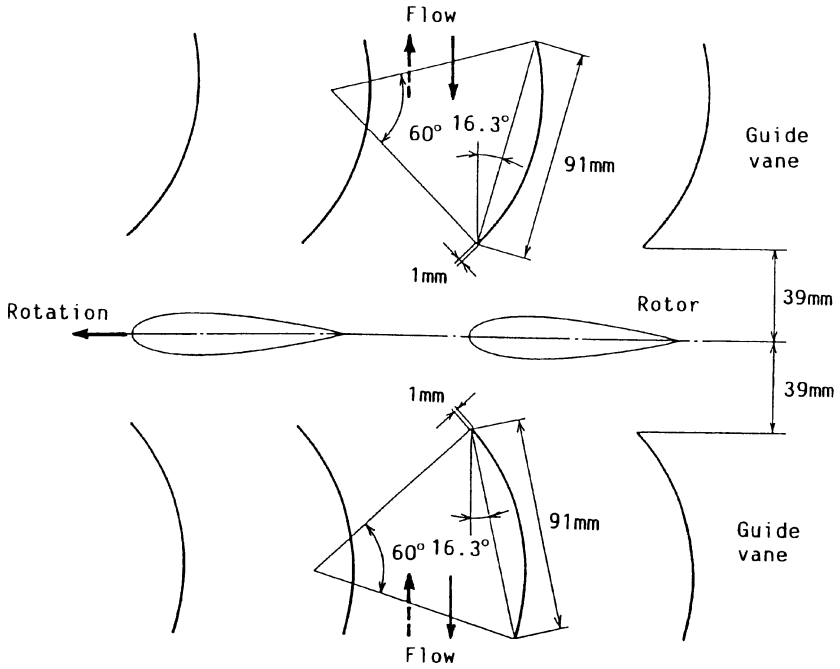

Figure 1. Wells turbine with guide vanes: WTGV.

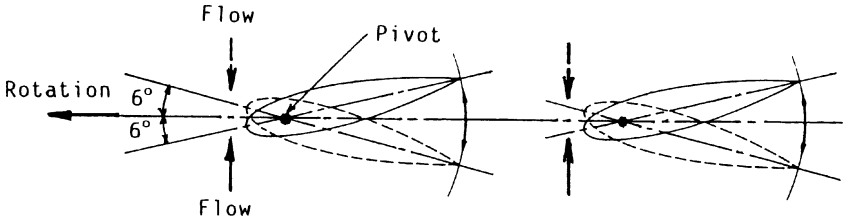

Figure 2. Turbine using self-pitch-controlled blades: TSCB.

the turbine angular velocity ω, the turbine output torque T_o, the flow rate Q and the total pressure drop between settling chamber and atmosphere Δp. The uncertainties in torque coefficient C_T and input coefficient C_A are $\pm 1\,\%$, respectively.

The details of turbines adopted in the experiment are as follows:

(a) Wells turbine with guide vanes, WTGV (*figure 1*); NACA0020, $AR = 0.5$, $l_r = 90$ mm, $\sigma_{rR} = 0.67$ and $\sigma_{gR} = 1.25$.

(b) Turbine with self-pitch-controlled blades, TSCB (*figure 2*); NACA0020, $AR = 0.5$, $l_r = 90$ mm, $\sigma_{rR} = 0.67$ and preset angle of 6°.

(c) Biplane Wells turbine with guide vanes, BWGV (*figure 3*); NACA0020, $AR = 0.5$, $l_r = 90$ mm, $\sigma_{rR} = 0.45$ and $\sigma_{gR} = 1.25$.

(d) Impulse turbine with self-pitch-controlled guide vanes, ISGV (*figure 4*); $t_a/S_r = 0.4$, $l_r = 54$ mm, $\gamma = 60°$, $\sigma_{rR} = 2.02$, $\sigma_{gR} = 2.27$, $\theta_1 = 17°$, $\theta_2 = 72.5°$ and $\lambda = -7.5°$.

(e) Impulse turbine with fixed guide vanes, IFGV (*figure 5*); $t_a/S_r = 0.4$, $l_r = 54$ mm, $\gamma = 60°$, $\sigma_{rR} = 2.02$, $\sigma_{gR} = 2.27$, $\theta = 30°$ and $\lambda = -7.5°$.

Note here that the configurations considered for these turbines are the ones found to be most promising in the previous studies [3–7]. Furthermore, all of them can start [12] by themselves.

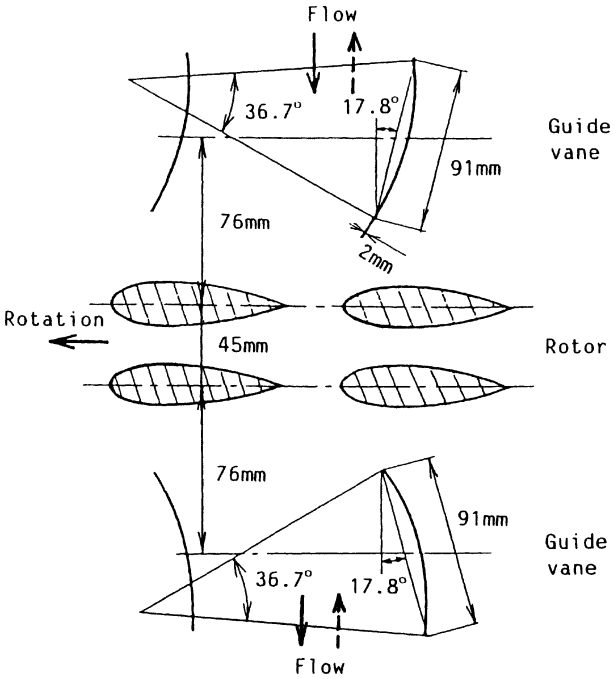

Figure 3. Biplane Wells turbine with guide vanes: BWGV.

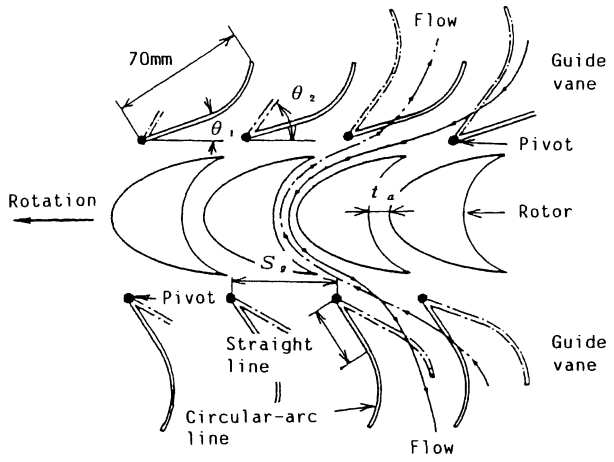

Figure 4. Impulse turbine with self-pitch-controlled guide vanes connected by link motion: ISGV.

3. TURBINE CHARACTERISTICS UNDER STEADY FLOW CONDITIONS

Turbine characteristics under steady flow condition were evaluated with torque coefficient C_T, input power coefficient C_A and flow coefficient ϕ, which are defined as:

$$C_T = T_o / \{\rho_a w^2 b l_r z r_R / 2\}, \quad (1)$$

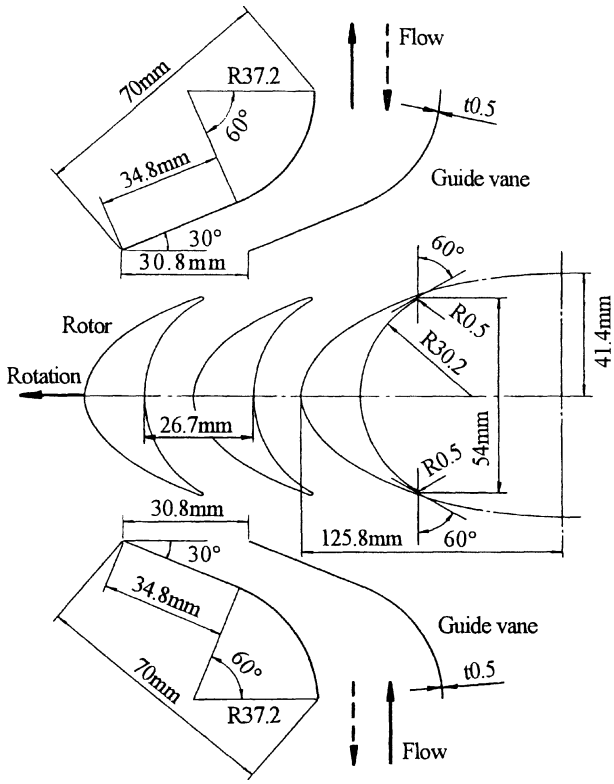

Figure 5. Impulse turbine with fixed guide vanes: IFGV.

$$C_A = \Delta p Q / \{\rho_a w^2 b l_r z v_a / 2\}, \quad (2)$$

$$\phi = v_a / U_R \quad (3)$$

where ρ_a—density of air, b—rotor blade height, l_r—chord length of rotor.

Figure 7(a) shows C_T–ϕ characteristics for the five turbines. Abrupt decreases in C_T characteristics due to rotor stall are observed for all the Wells type rotors such as WTGV, TSCB and BWGV. The value of ϕ where rotor stall starts is the largest for TSCB and the value of ϕ at $C_T = 0$ for TSCB is larger than other Wells type turbines. This is because relative inflow angle for rotor is lower than the case that rotor blades are fixed at 90 degrees of stagger angle. On the other hand, for both the impulse type rotors such as ISGV and IFGV, the value of C_T increases with increasing ϕ, and the value of C_T at region of large ϕ is larger than the Wells type turbines. The value of ϕ at $C_T = 0$ is larger than the Wells type turbines.

Figure 7(b) shows C_A–ϕ characteristics for the five turbines. The value of C_A for WTGV is the largest in the five turbines at any flow coefficient. This means that the pressure in air chamber is higher than other turbines and should be taken care for the maintenance

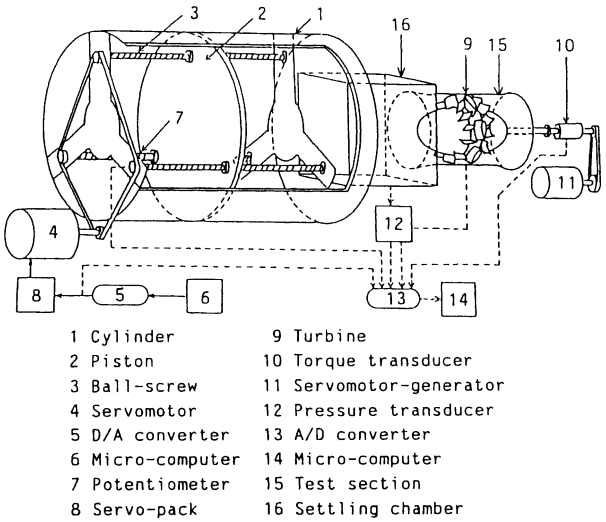

Figure 6. Test rig.

of bearing because of larger thrust force. On the other hand, for TSCB, BWGV, ISGV and IFGV, the value of C_A is rather small, especially for ISGV and IFGV. This means that the pressure increase in air chamber is small when impulse type turbines are adopted for wave power generator device.

Concerning the turbine efficiency η under steady flow conditions, we can easily take η–ϕ characteristics from *figure 7* because of $\eta = C_T/(C_A\phi)$. However, it should be noted that η does not give the useful information about the suitable turbine for wave power conversion. This is because turbine characteristics depend on the efficiency of air chamber, i.e., the ratio of power of OWC and incident wave power.

4. SIMULATION OF TURBINE CHARACTERISTICS UNDER IRREGULAR FLOW CONDITIONS

Since sea waves are irregular, and the airflow generated by the oscillating water column is also thus irregular, it is very important to clarify the turbine characteristics in connection with OWC under irregular flow conditions. Here let us simulate the characteristics in order to clarify the turbine for wave energy conversion.

The test irregular wave used in this study is based on the ISSC (International Ship Structure Congress) spectrum which is typical in the field of ocean engineering [13]. The spectrum is given as:

$$S^*(f^*) = 0.11 f^{*-5} \exp(-0.44 f^{*-4}) \qquad (4)$$

The incident wave height H is given as a function of time by such a spectrum. A typical example of wave height in dimensionless form $H^* = H/H_{1/3}$ is shown in *figure 8*, where the significant wave height $H_{1/3}$, the wave mean frequency $\overline{f}$ and the area ratio m are 1.0 m, 0.167 Hz and 0.0234, respectively.

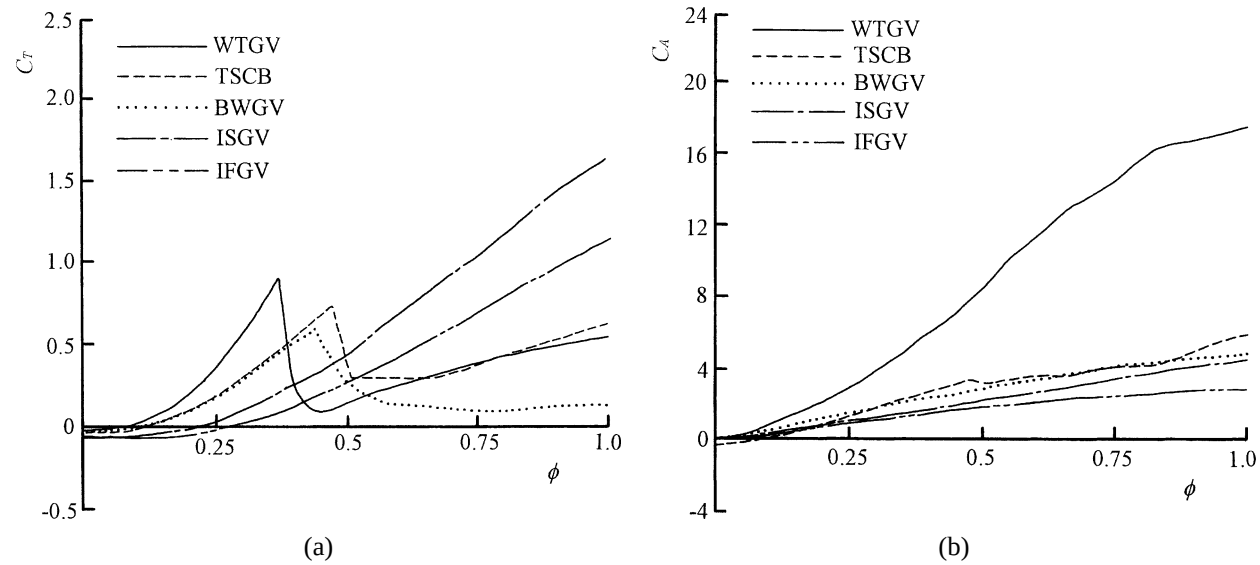

Figure 7. Comparison of turbine characteristics under steady flow conditions: (a) Torque coefficient; (b) Input coefficient.

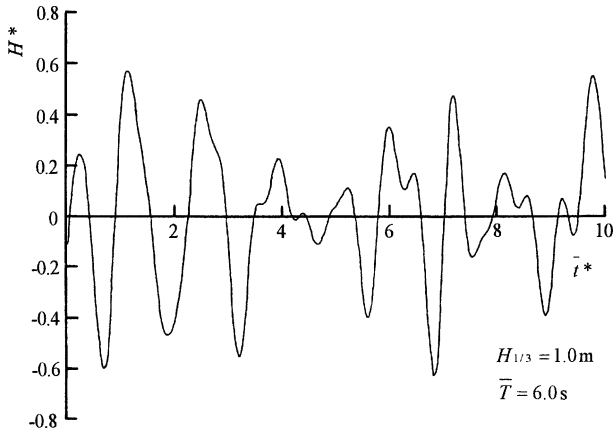

Figure 8. Test irregular wave.

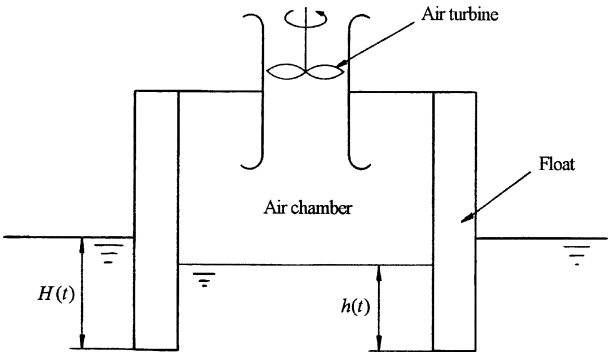

Figure 9. Schematic layout of OWC-air turbine type wave power generator system.

On the other hand, for a wave energy device as shown in *figure 9*, the relationship between the incident wave height and the wave height within air chamber [7] is given as:

$$\frac{\mathrm{d}}{\mathrm{d}t}\left(\rho_{\mathrm{s}} h A_{\mathrm{c}} \frac{\mathrm{d}h}{\mathrm{d}t}\right) = \left\{\rho_{\mathrm{s}} g(H-h) - \Delta p\right\} A_{\mathrm{c}} \qquad (5)$$

where ρ_{s}—density of seawater, A_{c}—air chamber cross-sectional area, g—gravity. Since $v_{\mathrm{a}} = \frac{1}{m}\frac{\mathrm{d}h}{\mathrm{d}t}$, Δp is a function of $\frac{\mathrm{d}h}{\mathrm{d}t}$ if the rotational speed U_{R} is given. This is approximate equation because the equation of motion about OWC is generally expressed by using linear water wave theory [14]. As the relationship between Δp and $\frac{\mathrm{d}h}{\mathrm{d}t}$ is obtained from C_{A}–ϕ characteristics, here let it put as $\frac{\Delta p}{\rho_{\mathrm{s}}} \equiv F(\frac{\mathrm{d}h}{\mathrm{d}t})$, equation (5) is rewritten as follows:

$$\rho_{\mathrm{s}} A_{\mathrm{c}}\left\{\left(\frac{\mathrm{d}h}{\mathrm{d}t}\right)^2 + h\frac{\mathrm{d}^2 h}{\mathrm{d}t^2}\right\} = A_{\mathrm{c}}\left\{\rho_{\mathrm{s}} g(H-h) - \Delta p\right\}$$

Then,

$$h\frac{\mathrm{d}^2 h}{\mathrm{d}t^2} + \left(\frac{\mathrm{d}h}{\mathrm{d}t}\right)^2 + F\left(\frac{\mathrm{d}h}{\mathrm{d}t}\right) - g(H-h) = 0 \qquad (6)$$

The above equation can be solved by using Runge–Kutta–Gill method, and then the wave height within air chamber is obtained. The incident wave power $\overline{W}_{\mathrm{i}}$ and power of OWC $\overline{W_{\mathrm{O}}}$ are defined as follows:

$$\overline{W}_{\mathrm{i}} = \sum_{i=1}^{N} \frac{1}{32\pi}\rho_{\mathrm{s}} g^2 H_{\mathrm{i}}^2 T_{\mathrm{i}}^2 / \sum_{i=1}^{N} T_{\mathrm{i}}, \qquad (7)$$

$$\overline{W}_{\mathrm{O}} = \sum_{i=1}^{N} \frac{1}{32\pi}\rho_{\mathrm{s}} g^2 h_{\mathrm{i}}^2 T_{\mathrm{i}}^2 / \sum_{i=1}^{N} T_{\mathrm{i}} \qquad (8)$$

Then, the efficiency of air chamber is

$$\tilde{\eta}_{\mathrm{c}} = \overline{W}_{\mathrm{O}} / \overline{W}_{\mathrm{i}} \qquad (9)$$

Note here that strictly speaking, pressure and flow rate of air should be taken into consideration for an evaluation of the efficiency of air chamber. However, the objective of this study is just to compare the performances of the turbines relatively. In this case, it is considered that above method is suitable to enough to evaluate the efficiency of the chamber. Therefore, a ratio of the power of OWC to the incident wave power has been adopted as the efficiency.

Assuming incompressible flow, the axial flow velocity is directly proportional to a variation of the wave height. The nondimensional axial flow velocity through the turbine v_{a}^* is written as:

$$v_{\mathrm{a}}^* = \frac{\mathrm{d}(h/H_{1/3})}{\mathrm{d}(t/\overline{T})} = \frac{\mathrm{d}h^*}{\mathrm{d}\overline{t}^*} \qquad (10)$$

The running and starting characteristics of the turbine in irregular flow were calculated by numerical simulation. The steady flow characteristics of the turbines are assumed to be valid for computing performance under unsteady flow conditions. Such a quasi-steady analysis has been validated by the previous studies for both Wells turbine [15] and the impulse turbine [16].

The equation of motion for a rotating system of the turbine in irregular flow can be described in dimensionless form as:

$$K^2 X_{\mathrm{I}} \frac{\mathrm{d}\overline{\omega}^*}{\mathrm{d}\overline{t}^*} + X_{\mathrm{L}} = C_{\mathrm{T}}(\phi)\frac{(K\overline{\omega}^*)^2 + v_{\mathrm{a}}^{*2}}{2}\sigma_{\mathrm{rR}}\frac{4(1-\nu)}{1+\nu} \qquad (11)$$

where $\phi = v_{\mathrm{a}}^*/(K\overline{\omega}^*)$, $K\overline{\omega}^* = \omega m r_{\mathrm{R}}\overline{T}/H_{1/3}$ and $v_{\mathrm{a}}^* = m\overline{T}v_{\mathrm{a}}/H_{1/3}$. The first and second terms on the left side of

equation (11) are inertia and loading terms, respectively, and the right hand side represents a torque generated by a turbine. It is clear from equation (11) that the behavior of the turbine (starting characteristics) can be calculated as a function of $K\overline{\omega}^*$ and v_a^*, when loading characteristics $X_L(\overline{\omega}^*)$, torque coefficient $C_T(\phi)$ and rotor geometrical parameters such as X_I, σ_{rR} and ν are specified.

Similarly, the running characteristics are obtained by keeping rotational speed constant. In this case, the mean output $\overline{C}_o$ and input coefficient $\overline{C}_i$ from $t^* = 0$–10 (see *figure 8*) are given respectively as:

$$\overline{C}_o = \frac{1}{\overline{t}^*}\int_0^{t^*} C_T(\phi)\frac{(K\overline{\omega}^*)^2 + v_a^{*2}}{2} \times \sigma_{rR}\frac{4(1-\nu)}{1+\nu}\overline{\omega}^*\,\mathrm{d}\overline{t}^* \qquad (12)$$

$$\overline{C}_i = \frac{1}{\overline{t}^*}\int_0^{t^*} C_A(\phi)\frac{(K\overline{\omega}^*)^2 + v_a^{*2}}{2K} \times \sigma_{rR}\frac{4(1-\nu)}{1+\nu}v_a^*\,\mathrm{d}\overline{t}^* \qquad (13)$$

Then, mean turbine efficiency is

$$\tilde{\eta}_t = \overline{C}_o/\overline{C}_i \qquad (14)$$

Therefore, the conversion efficiency of the wave energy device is

$$\tilde{\eta} = \tilde{\eta}_c \cdot \tilde{\eta}_t \qquad (15)$$

In the calculations, the flow condition is assumed to be quasi-steady, therefore, the values of C_T and C_A shown in *figure 7* can be used here. For simplifying the numerical simulation of ISGV, pitch angle of guide vanes are assumed to change at the same time when axial velocity changes from positive to negative (or from negative to positive). The validity of this assumption was shown by [6], in which calculation of maximum turbine efficiency and starting characteristics agreed with the experimental data. For the numerical simulation of TSCB, based on the experimental data by [17], pitch angle of rotor is assumed to change into $\gamma = 6$ degrees for $\phi \geq 0.37$ and remain $\gamma = 0$ degree for $\phi < 0.37$.

Figure 10 shows the comparison of conversion efficiency of wave energy. For the impulse type turbines, conversion efficiency is quite high at region of large $1/(K\overline{\omega}^*)$ compared with the Wells type turbines. Especially, the value of maximum efficiency for ISGV is about 47% and over 15% larger than that of WTGV which is now mainly used for wave power conversion. Since rotor stall does not occur for the impulse type turbine as shown

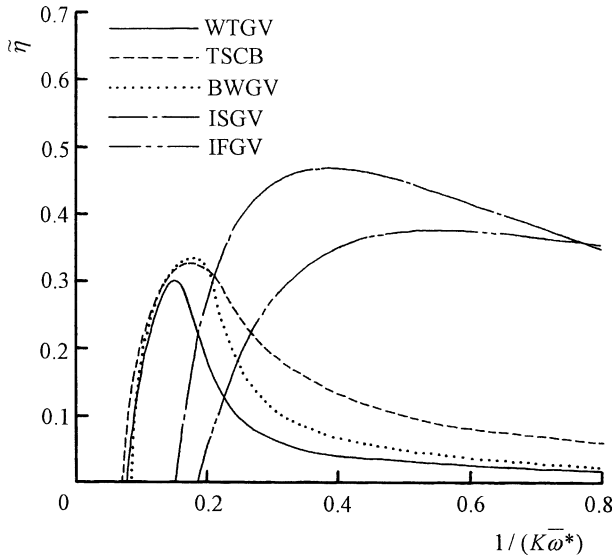

Figure 10. Comparison of conversion efficiency of wave energy.

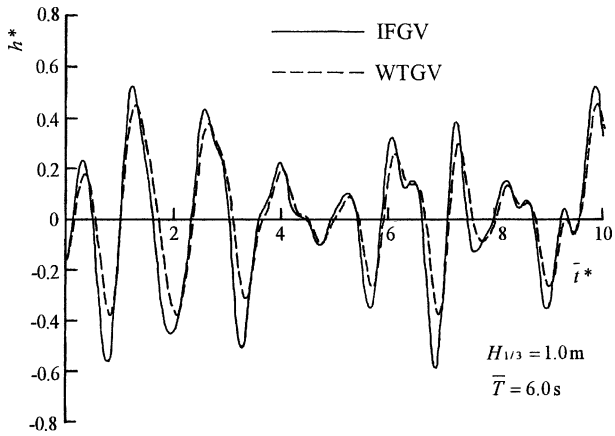

Figure 11. Time variations of wave height in air chamber at condition showing maximum efficiency.

in *figure 7(a)*, torque can be obtained with comprehensive region of flow coefficient. Although ISGV has a disadvantage of maintenance of pivots, even for IFGV, where guide vanes are fixed for simple configuration, the maximum efficiency of IFGV is larger than that of WTGV by about 6%. Therefore, it is no doubt that the impulse type turbine has better running characteristics than the Wells type turbine. Here note that this tendency is almost the same for any $H_{1/3}$.

Figure 11 shows time variation of wave height in air chamber at condition showing maximum efficiency for WTGV and IFGV. The maximum value of h^* for IFGV is larger than that for WTGV. Since the value

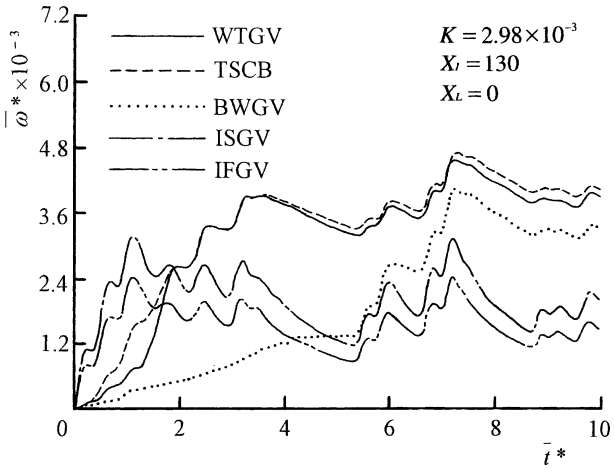

Figure 12. Starting characteristics under irregular wave conditions.

of C_A for WTGV is large as shown in *figure 7(b)*, the pressure in air chamber become high and the motion of OWC is suppressed. For IFGV, however, the motion of OWC is more active because the value of C_A is lower and rotational speed of rotor is quite lower than that of the Wells turbine. Therefore, the difference of the efficiency of air chamber is considered to be one of cause that energy conversion efficiency of wave power conversion using the impulse type turbine is higher than that efficiency using the Wells type turbine.

The starting characteristics for five turbines are shown in *figure 12*. The impulse type turbine can start in very short time. This fact means that a generating time of a generator with the impulse turbine is longer than that of the Wells turbine. Furthermore, the rotational speed at operation is much smaller than those of the Wells type turbines. These are because the torque coefficient C_T of the impulse type turbine is higher than that of the Wells turbine, and the flow coefficient at loading-free condition for the impulse turbine is larger than the Wells type turbines as shown in *figure 7(a)*. Therefore, it is possible for the impulse type turbines to design an excellent turbine with low operational speed, which is desirable from the viewpoints of noise reduction and mechanical advantage.

5. CONCLUSIONS

The characteristics of self-rectifying air turbines for wave power conversion proposed so far have been investigated by the model testing and numerical simulation under irregular flow conditions. As a result, the impulse type turbines have the potential to be superior to the Wells type turbines in the overall performances under irregular flow conditions. This is because the impulse turbine has no rotor stall and the operational speed is very low.

REFERENCES

[1] Inoue M., Kaneko K., Setoguchi T., Saruwatari T., Studies on the Wells turbine for wave power generator (turbine characteristics and design parameter for irregular wave), JSME Internat. J. Ser. II 31 (4) (1988) 676–682.

[2] Raghunathan S., Tan C.P., Performance of Wells turbine at starting, J. Energy 6 (1982) 430–431.

[3] Setoguchi T., Takao M., Kaneko K., Inoue M., Effect of guide vanes on the performance of a Wells turbine for wave energy conversion, Internat. J. Offshore Polar Engrg. 8 (2) (1998) 155–160.

[4] Inoue M., Kaneko K., Setoguchi T., Hamakawa H., Air turbine with self-pitch-controlled blades for wave power generator (estimation of performances by model testing), JSME Internat. J. Ser. II 32 (1) (1989) 19–24.

[5] Setoguchi T., Kaneko K., Hamakawa H., Inoue M., Some techniques to improve the performance of biplane Wells turbine for wave power generator, in: Proceedings of 1st Pacific/Asia Offshore Mechanics Symposium, The International Society of Offshore and Polar Engineers, Seoul, Korea, Vol. 1, 1990, pp. 207–212.

[6] Setoguchi T., Kaneko K., Taniyama H., Maeda H., Inoue M., Impulse turbine with self-pitch-controlled guide vanes connected by links, Internat. J. Offshore Polar Engrg. 6 (1) (1996) 76–80.

[7] Setoguchi T., Takao M., Kinoue Y., Kaneko K., Inoue M., Study on an impulse turbine for wave energy conversion, in: Proceedings of 9th International Offshore and Polar Engineering Conference, The International Society of Offshore and Polar Engineering, Brest, France, Vol. 1, 1999, pp. 180–187.

[8] Miyazaki T., Utilization of coastal seas by floating wave energy device 'Mighty Whale', in: Proceedings of European Wave Energy Symposium, Edinburgh, UK, 1993, pp. 373–378.

[9] Falcao A.F.O., Whittaker T.J.T., Lewis A.W., JOULE II preliminary action: European pilot plant study, in: Proceedings of European Wave Energy Symposium, Edinburgh, UK, 1993, pp. 247–257.

[10] Santhakumar S., Report of workshop on turbine for ocean energy application, Indian Institute of Technology, Madras, India, 1996.

[11] Thakker A., Frawley P., Khaleeq H.B., Private communication with wave energy research team, University of Limerick, Ireland, 1999.

[12] Inoue M., Kaneko K., Setoguchi T., Raghunathan S., Simulation of starting characteristics of the Wells turbine, AIAA/ASME 4th Fluid Mech Plasma Dynamics Laser Conference, AIAA-86-1122, 1986.

[13] Hineno M., Yamauchi Y., Spectrum of sea wave, J. Soc. Nav. Arch. Japan 609 (1980) 160–180 (in Japanese).

[14] Chatry G., Clement A.H., Sarmento A.J.N.A., Simulation of a self-adaptively controlled OWC in a nonlinear wave tank, in: Proceedings of 9th International Offshore and

Polar Engineering Conference, The International Society of Offshore and Polar Engineers, Brest, France, Vol. 3, 1999, pp. 290–296.

[15] Inoue M., Kaneko K., Setoguchi T., Shimamoto K., Studies on Wells turbine for wave power generator (part 4; starting and running characteristics in periodically oscillating flow), Bull. JSME 29 (250) (1986) 1177–1182.

[16] Setoguchi T., Kaneko K., Maeda H., Kim T.W., Inoue M., Impulse turbine with self-pitch-controlled guide vanes for power conversion: performance of mono-vane type, Internat. J. Offshore Polar Engrg. 3 (1) (1993) 73–78.

[17] Takao M., Setoguchi T., Kaneko K., Inoue M., Air turbine with self-pitch-controlled blades for wave energy conversion, Internat. J. Offshore Polar Engrg. 7 (4) (1997) 308–312.